

DOI: 10.1002/adfm.200800566

Synthesis of Polymerizable Superoxide Dismutase Mimetics to Reduce Reactive Oxygen Species Damage in Transplanted Biomedical Devices**

By Charles Y. Cheung, Suzanne J. McCartney, and Kristi S. Anseth*

A new polymerizable superoxide dismutase (SOD) mimetic metalloporphyrin macromer was synthesized to minimize inflammatory damage associated with tissue transplantation and biomaterial implantation, such as the use of encapsulated pancreatic islets for the treatment of type I diabetes mellitus (T1DM). This functional SOD mimetic, Mn(III) Tetrakis[1-(3-acryloxy-propyl)-4-pyridyl] porphyrin (MnTPPyP-Acryl), was copolymerized and crosslinked with poly(ethylene glycol) diacrylate (PEGDA) to form hydrogel networks that may actively reduce reactive oxygen species (ROS) damage associated with biomaterial implantation. Solution phase activity assays with MnTPPyP-Acryl macromers showed comparable SOD activity to MnTMPyP, a non-polymerizable commercially available SOD mimetic. This work also describes the development of a new, simple, and inexpensive solid phase assay system that was developed to assess the activity of MnTPPyP-Acryl macromers polymerized within PEGDA hydrogels, which has the potential to fulfill an existing void with the biochemical tools available for testing other immobilized ROS antagonists. With this new assay system, hydrogels containing up to 0.25 mol% MnTPPyP-Acryl showed significantly higher levels of SOD activity, whereas control hydrogels polymerized with inactive TPPyP-Acryl macromers showed only background levels of activity. The potential for repeated use of such hydrogel devices to consistently reduce superoxide anion concentrations was demonstrated upon retention of ~100% SOD activity for at least 72 h post-polymerization. These results demonstrate the potential that polymerizable SOD mimetics may have for integration into medical devices for the minimization of inflammatory damage upon transplantation, such as during the delivery of encapsulated pancreatic islets.

1. Introduction

Type I diabetes mellitus (T1DM) is an autoimmune disease in which the insulin-producing β -cells comprising the islets of Langerhans in the pancreas are destroyed, resulting in the loss of insulin production. Pancreatic islet cell transplantation represents a promising new treatment option for T1DM, providing concurrent glucose sensing and insulin producing capabilities. Encapsulating pancreatic islets in cell-impermeant passive biomaterial matrices may provide protection for the transplanted islets from autoimmune reactivity without the need for administering immunosuppressive drugs. These passive biomaterial barrier systems physically prohibit the migration of cells into the encapsulation devices, thereby preventing immune cell contact-mediated destruction to the transplanted cells. However, these passive barrier devices cannot prevent diffusion of small molecule toxins, such as certain cytokines and reactive oxygen species (ROS), produced by activated immune cells from penetrating through the

polymeric barriers and damaging the encapsulated tissue. Release of ROS, such as superoxide anions, hydrogen peroxide (H_2O_2), nitric oxide (NO^\bullet), and other reactive nitrogen species by macrophages and neutrophils may be involved in β -cell damage and destruction during insulinitis, a pre-diabetic stage characterized by inflammation of the pancreas.^[1,2] ROS toxicity is associated both with direct oxidative damage of proteins, lipids (i.e., membrane lipid peroxidation) and DNA, but also with the ability of ROS to act as second messengers that ultimately lead to increased inflammatory cytokine production and autoimmune responses, such as pro-inflammatory $\text{NF}\kappa\text{B}$ activation.^[3]

Many deleterious effects are associated with the presence of superoxide anions. For example, superoxide anions are highly reactive and can react with nitric oxide to form peroxynitrite (ONOO^-), a pro-inflammatory and cytotoxic reactive molecule that can increase neutrophils adhesion and infiltration, as well as regulate the release of certain cytokines.^[4] Mammalian cells have evolved protective enzymes, such as superoxide dismutases (SODs), which catalyze the degradation of superoxide anions to less reactive H_2O_2 and oxygen, as shown in Equation (1)



Cells can be exposed to both intracellular and extracellular sources of superoxide anions, therefore, SOD enzymes are

[*] Prof. K. S. Anseth, Dr. C. Y. Cheung, S. J. McCartney
Department of Chemical and Biological Engineering and the Howard Hughes Medical Institute
University of Colorado, Boulder, CO 80309-0424 (USA)
E-mail: kristi.anseth@colorado.edu

[**] This work was partially supported by the NSF (EEC0444771).

present both intracellularly and extracellularly to counteract cellular exposure to superoxide anions from these different sources. In acute and chronic inflammation, the rate of superoxide anion production increases to levels beyond which endogenous SOD enzymes cannot sustainably remove, resulting in superoxide-related tissue damage.^[5]

Although native SOD enzymes are extremely efficient at dismutating superoxide anions, effective therapies utilizing native SOD enzymes may be problematic due to concerns with protein instability, short circulation half-lives, and potential antigenicity,^[4] leading to the development of various SOD mimetics (SODm). SOD mimetics are small organic molecules that mimic the catalytic activity of SOD enzymes without the limitations associated with native SOD enzymes. SOD mimetics have broad antioxidant properties, including superoxide, H₂O₂, peroxynitrite, nitric oxide, and lipid peroxyl free radical scavenging.^[4,6] Most mimetics are designed with an active redox metal center coordinated within a central carbon-based ring structure. Several manganic porphyrins have shown SOD activity, with the catalytic activity of Mn(III) Tetrakis(1-methyl-4-pyridyl) porphyrin (MnTMPyP) among the highest of the manganic porphyrins,^[7] and reported to be between 1 and 3% of native SOD enzyme activity.^[8] In addition, *in vivo* studies with MnTMPyP administered to streptozotocin-induced diabetic Wistar rats decreased animal mortality and increased the lifespan of rats, presumably due to the antioxidant capabilities of this SODm.^[9]

Patients with T1DM have been shown to have defects with their antioxidant protection mechanisms.^[3] Several key enzymes that normally reduce oxidative stress are present at extremely low levels in pancreatic islet tissue compared to surrounding tissue, such as Mn and Cu/Zn SOD found intracellularly, extracellular SOD (EC-SOD), catalase, and glutathione peroxidase, thereby making islets more susceptible to damage associated with ROS.^[3,10,11] Superoxide anions can be secreted by infiltrating macrophages into post-islet transplantation sites, which may contribute to β -cell damage.^[12,13] Therefore, methods developed to neutralize this secreted form of superoxide anions prior to them damaging transplanted islets would be beneficial. Investigators have shown that exogenously administered SOD enzyme protected mouse pancreatic islets *in vivo* from the onset of diabetes induced by alloxan, a chemical known to mediate the production of ROS, indicating that high levels of EC-SOD were required to protect islets from alloxan-mediated damage.^[14] Parental injections of PEG-conjugated Cu/Zn-SOD protected both endogenous and transplanted islets in NOD mice.^[15,16] In addition, extracellularly generated oxygen free radicals have the potential to damage the plasma membranes of β -cells, and administration of SOD enzyme mitigated the damage incurred to β -cells *in vitro*.^[17]

Recently, we have developed methodologies to transform passive biomaterial barriers into active barrier systems that may either promote encapsulated islet cell survival or proactively protect encapsulated islets from immune-mediated damage.^[18,19] In this work, we aim to prepare active barrier

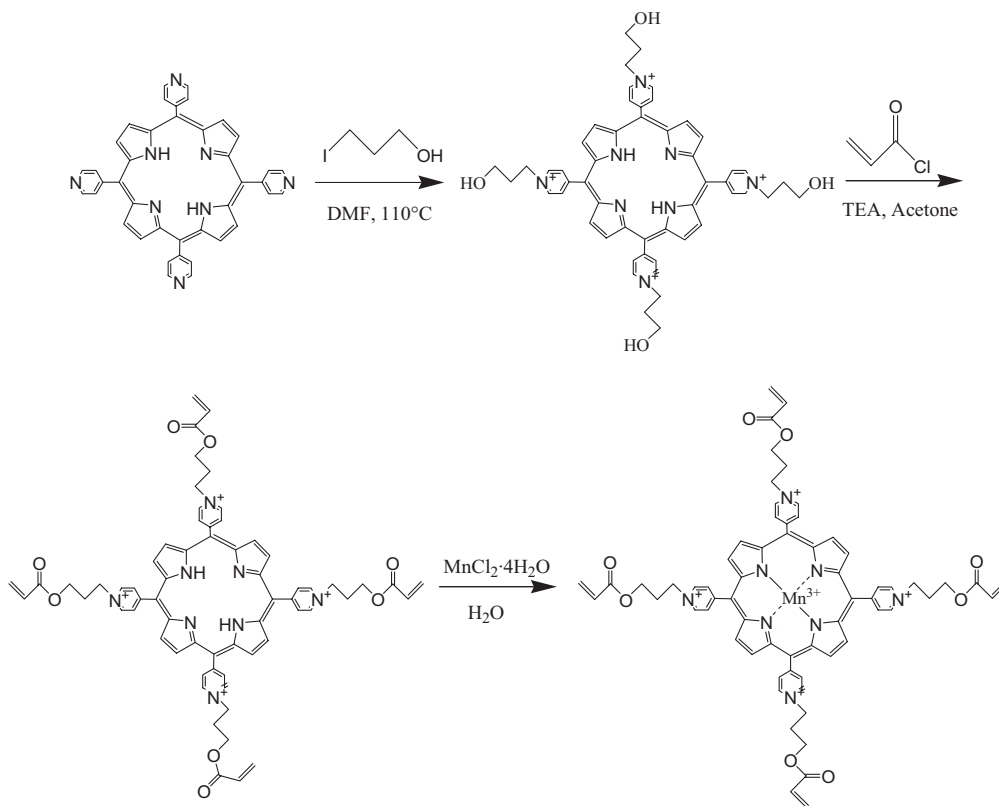
systems that can reduce inflammatory damage due to ROS secreted by activated innate immune cells in response to tissue graft transplantation. Polymerization of SOD mimetics within these hydrogel barriers will provide localized protection of encapsulated cells from ROS-mediated damage, and therefore should preclude the need for systemically administered immunosuppressive therapeutics to mitigate ROS damage. We describe the novel synthesis of a polymerizable metalloporphyrin that was structurally similar to a commercially available SOD mimetic, MnTMPyP, which retained high levels of SOD activity. We then demonstrate the ability to photopolymerize this SOD mimetic into poly(ethylene glycol)diacrylate (PEGDA) hydrogels. In addition, a unique, simple and inexpensive solid-phase assay was developed to assess the activity of the SOD mimetic polymerized within this hydrogel matrix, which has the potential to serve as a useful biochemical tool which is currently lacking for testing the activity of immobilized ROS antagonists.

2. Results and Discussion

Previous research into porphyrin modification has focused on either the immobilization of non-metallo porphyrins onto polymeric supports to serve as catalysts for organic syntheses^[20,21] to study protein binding/adsorption,^[22] or for free radical polymerization of non-metallo porphyrins into linear polymer chains to study oxygen transport.^[23–26] SOD mimetic metalloporphyrins have also been conjugated onto linear polymers to increase circulation half-lives and bioavailability of their compounds, but retained only minimal levels of activity (i.e., ~0.1%) compared to the activity of native SOD enzyme.^[27,28] The work herein describes the creation of a polymerizable SOD mimetic that has the potential to be incorporated into any polymer system capable of formation by free radical polymerization, with retention of high levels of SOD mimetic activity.

2.1. Synthesis of MnTPPyP-Acryl

A new SOD mimetic containing polymerizable acrylate groups, Mn(III) Tetrakis[1-(3-acryloxy-propyl)-4-pyridyl] porphyrin (MnTPPyP-Acryl), was designed and synthesized based upon MnTMPyP, a commercially available SOD mimetic that is an effective antioxidant,^[8] for immobilization into solid-phase hydrogel networks. In our synthetic scheme, the base structure of the porphyrin was kept intact to allow for proper coordination of Mn ions, which are integral to maintaining SOD activity, while the pyridyl groups were modified to provide the polymerizable acrylate groups. In this multi-step synthesis scheme (Scheme 1), meso-Tetra(4-pyridyl)porphine (TPyP) was quarternized with 3-iodopropanol to both produce the cationic pyridyl groups that are necessary to confer SOD activity to the molecule,^[29] as well as provide hydroxyl groups for further reactivity. The



Scheme 1. Synthesis of TPPyP-OH, TPPyP-Acryl, and MnTPPyP-Acryl.

hydroxylated, cationic base porphyrin was then acrylated by reacting with acryloyl chloride. ^1H NMR verified quarterization and acrylation of TPyP, with approximately 82 and 66% of the four pyridyl groups per molecule quarterized and subsequently acrylated, respectively. In the final synthesis step, the acrylated cationic meso-Tetra[1-(3-acryloxy-propyl)-4-pyridyl] porphine (TPPyP-Acryl) was metallated with $\text{MnCl}_2 \cdot 4\text{H}_2\text{O}$ to coordinate the Mn(III) core within the pyrrole center of the molecule to provide SOD activity. Full metallation of the porphyrin was verified by observing the concomitant Soret band shift from 424 to 463 nm, from TPPyP-Acryl to MnTPPyP-Acryl, which is characteristic of MnTPPyP^[8] (Fig. 1). The absorbance spectrum from 300 to 600 nm for both MnTPPyP and MnTPPyP-Acryl were similar, which is indicative that the synthesized MnTPPyP-Acryl retained similar structural elements as the MnTPPyP, as expected.

2.2. Activity Assay with Xanthine/Xanthine Oxidase System

The SOD activity of MnTPPyP-Acryl macromers was quantified using the standard xanthine/xanthine oxidase assay system first developed by McCord and Fridovich.^[30] Superoxide anion generation by the xanthine/xanthine oxidase system was quantified by measuring cytochrome *c* reduction at 550 nm. Typical absorbance plots generated for MnTPPyP-

Acryl and MnTPPyP SOD mimetics at concentrations ranging from 0 to 500 nm are shown in Figure 2. From these plots, the concentration of MnTPPyP-Acryl and MnTPPyP that provided one unit of SOD activity as defined by McCord and Fridovich^[30] was calculated at approximately 130 and 140 nM, respectively. Analysis of these data provided the units of SOD activity for native SOD enzyme, MnTPPyP, and MnTPPyP-Acryl, and are displayed in Table 1 on both a per mass and

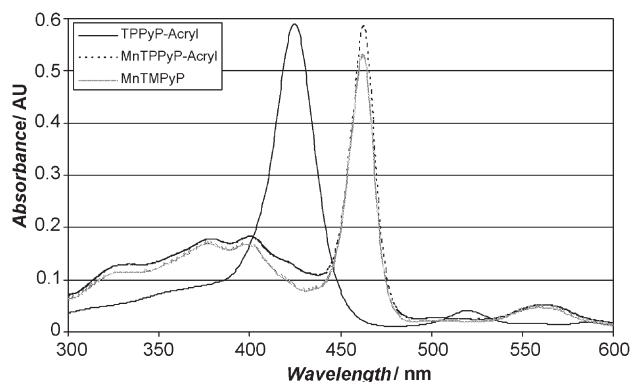


Figure 1. Absorbance spectra for porphyrin compounds between 300 and 600 nm. Spectral traces were for solutions prepared at 2.5 μM (TPPyP-Acryl) and 5 μM (MnTPPyP-Acryl and MnTPPyP). The concomitant Soret band shift was observed from 424 nm (TPPyP-Acryl) to 463 nm (MnTPPyP-Acryl) upon porphyrin metallation. Comparable traces are observed for both MnTPPyP-Acryl and MnTPPyP, indicating structural similarity between conjugated electron structures.

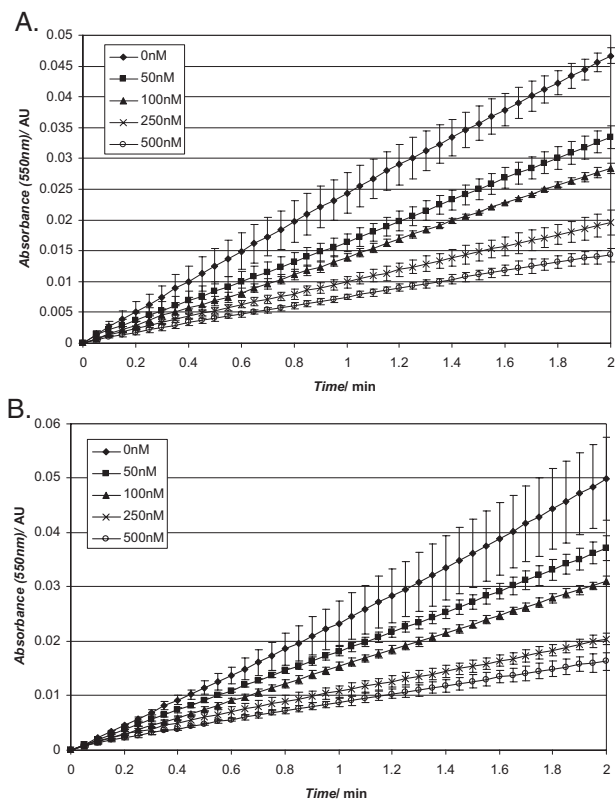


Figure 2. Representative graphs of solution-based SOD activity assays for A) MnTPPyP-Acryl and B) MnTPPyP using cytochrome *c* detection of superoxide anions generated by the xanthine/xanthine oxidase system. Concentrations of MnTPPyP-Acryl and MnTPPyP ranged from 0 to 500 nM. Absorbance changes monitoring increase in cytochrome *c* (reduced) concentration were measured at 550 nm for 2 min. All concentrations of MnTPPyP-Acryl were tested with $n = 3$ replicates.

per mol basis. From these data, both MnTPPyP and MnTPPyP-Acryl were twice as active as the native Cu/Zn SOD enzyme on a per mass basis due to their lower molecular weights. In contrast, the SOD enzyme had an approximately 20-fold higher activity level than either SOD mimetic on a molar level, indicating that SOD enzyme is more efficient at superoxide anion dismutation than either mimetic, which is similar to the findings by other investigators. Catalytic rate

Table 1. Solution-based SOD unit activity comparison between MnTPPyP-Acryl macromer, the commercially available SOD mimetic MnTPPyP, and native SOD enzyme using the xanthine/xanthine oxidase superoxide anion generation method with cytochrome *c* detection.

Molecule	Units mg^{-1}	Units μmol^{-1}
MnTPPyP-Acryl	11 000 \pm 1200	15 000 \pm 1500
MnTPPyP	15 000 \pm 720	14 000 \pm 650
SOD enzyme	8200 \pm 450	270 000 \pm 15 000

One unit of SOD activity was defined as the quantity of SOD or SODm required to reduce the absorbance of cytochrome *c* by $0.025 \text{ AU min}^{-1}$ at 550 nm.

constants were calculated for the reaction between native SOD enzyme or SOD mimetics (i.e., MnTPPyP and MnTPPyP-Acryl).^[31] Comparison of the initial rates of cytochrome *c* reduction in the absence (V) and presence (v) of either SOD enzyme or SOD mimetics lead to the following kinetic equation shown in Equation (2):

$$\frac{V}{v} = 1 + \frac{k_{\text{cat,SOD}}[\text{SOD}]}{k_{\text{cytc}}[\text{cyt } c(\text{ox})]} \quad (2)$$

where $k_{\text{cat,SOD}}$ is the initial rate constant of superoxide anion dismutation by SOD or SODm, k_{cytc} is the initial rate constant of cytochrome *c* reduction in the absence of SOD or SODm, $[\text{SOD}]$ is the concentration of SOD enzyme or SODm, and $[\text{cyt } c(\text{ox})]$ is the concentration of the oxidized form of cytochrome *c*. Therefore, $k_{\text{cat,SOD}}/\text{SODm}$ can be calculated as the slope from plots of SOD/SODm concentration versus V/v , utilizing a $k_{\text{cytc}} = 5.6 \times 10^5 \text{ M}^{-1} \text{ s}^{-1}$.^[32] From this relationship, the following catalytic rate constants were obtained: $k_{\text{cat,MnTPPyP}} = 3.5 (\pm 0.11) \times 10^7 \text{ M}^{-1} \text{ s}^{-1}$; $k_{\text{cat,MnTPPyP-Acryl}} = 3.1 (\pm 0.20) \times 10^7 \text{ M}^{-1} \text{ s}^{-1}$; and $k_{\text{cat,SOD}} = 2.7 (\pm 0.19) \times 10^9 \text{ M}^{-1} \text{ s}^{-1}$. These catalytic rate constants were comparable to previously reported rate constants for both MnTPPyP^[7,8] and native SOD enzyme.^[33] These data verified that MnTPPyP-Acryl maintained comparable SOD activity to the commercially available MnTPPyP SOD mimetic, indicating that chemical alteration of the methyl group connected to the quarternized pyridyl moieties on the metalloporphyrin to a longer-chain propyl acrylate moiety did not significantly alter the SOD activity of this molecule.

2.3. Functionalization of PEG Hydrogels

Photopolymerization of thick PEGDA hydrogels ($\sim 3.2 \text{ mm}$) was achieved containing up to 2 mol% MnTPPyP-Acryl. Figure 3 shows a representative image for larger diameter hydrogels prepared with 0–2 mol% MnTPPyP-Acryl. Any unreacted sol fraction of monomers was leached out of the gels prior to analysis. A higher degree of incorporation of MnTPPyP-Acryl was evident in hydrogel solutions loaded with increasing quantities of MnTPPyP-Acryl, as demonstrated by the increasing degree of opacity observed with these hydrogels. We attempted to polymerize

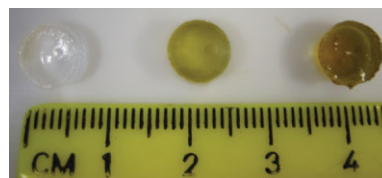


Figure 3. Digital images of 10 wt % PEGDA hydrogels polymerized with A) 0.5 mol%, B) 1 mol%, and C) 2 mol% MnTPPyP-Acryl. PEGDA/MnTPPyP-Acryl hydrogels were polymerized in Teflon molds for 10 min at 365 nm, and subsequently swollen for 1 h in PBS.

thick hydrogels with even higher percentages MnTPPyP-Acryl; however light attenuation at 365 nm through our gel solutions loaded at higher quantities of MnTPPyP-Acryl prevented sufficient gelation from occurring.

2.4. Rheological Measurements

Real-time measurements of the elastic modulus (G') and viscous modulus (G'') were recorded during the photopolymerization process for thin (50 μm) hydrogels containing MnTPPyP-Acryl. Polymerization of relatively thin hydrogels provided the capability to determine the influence of MnTPPyP-Acryl on polymerization reaction kinetics and ultimate hydrogel formation and final properties, while minimizing the effects of light attenuation by MnTPPyP-Acryl through the solution. Values for the crossover point for gelation for hydrogels (i.e., an estimate of the gel point conversion) containing up to 5 mol% MnTPPyP-Acryl are shown in Table 2. These data indicate that longer crossover times were obtained for solutions containing higher contents of MnTPPyP-Acryl, which most likely was due to light absorption by MnTPPyP-Acryl at 365 nm that results in light attenuation at increasing concentrations of MnTPPyP-Acryl, and therefore longer times were required for sol-to-gel transition. Crosslinking densities calculated for PEGDA/MnTPPyP-Acryl hydrogels from Equation (3) and are shown in Table 2. The final crosslinking densities for hydrogels containing 0.5 mol% MnTPPyP-Acryl were not statistically different from control PEGDA hydrogels lacking MnTPPyP-Acryl based on a Student's t -test (p -value > 0.1), indicating that low quantities of MnTPPyP-Acryl did not significantly influence or perturb the final hydrogel structure. However, MnTPPyP-Acryl concentrations at or above 1 mol% gradually reduced the degree of crosslink formation once the hydrogels were fully polymerized, indicating that higher quantities of MnTPPyP-Acryl in solution did affect the properties of the final hydrogels formed.

Table 2. The crossover point and final crosslinking density as calculated from the rheological properties of 10 wt% PEGDA networks ($MW = 10\,000\text{ g mol}^{-1}$) copolymerized with varying concentrations of MnTPPyP-Acryl macromer.

MnTPPyP-Acryl [mol%]	Crossover point [s]	ρ_x [mm]
0	73 \pm 1.3	6.3 \pm 0.26
0.5	80 \pm 3.0	6.5 \pm 0.15
1	90 \pm 0.9	5.9 \pm 0.021
2	109 \pm 2.4	4.9 \pm 0.16
3	129 \pm 5.0	4.1 \pm 0.041
4	153 \pm 5.0	3.6 \pm 0.026
5	197 \pm 1.7	3.0 \pm 0.10

In general, increasing functionalization led to inhibition of gelation and an optimal final crosslinking density existed at ~ 0.5 – 1.0 mol% MnTPPyP-Acryl.

2.5. Solid-Phase Assay of Functionalized SODm Hydrogel Activity

Inherent difficulties were evident when attempting to apply solution-based SOD activity assays to covalently attached SOD mimetics within 3-D matrices. Most of the widely utilized and easily applied assays for quantifying SOD activity rely on competition between a chromophore, such as ferricytochrome c or NBT, and SOD or SOD mimetics for solution phase reactivity with superoxide anions to measure the level of SOD activity.^[34] In contrast, immobilization of SOD enzymes or mimetics into 3-D environments prevents solution phase competition with the chromophore for superoxide anion reactivity in these standard assays by introducing a diffusion component required for proper SOD dismutation activity. The solid-phase nature of immobilized SOD enzymes and mimetics, combined with the extremely short half-life associated with superoxide anions prevents current assay systems from providing an accurate measurement of encapsulated SOD enzymes or mimetic dismutase activity. These limitations with current assay systems required us to develop a new solid phase assay capable of assessing the activity of SOD mimetics polymerized within a 3-D environment, such as the mimetics polymerized within our hydrogels. Due to the short-lived nature of the superoxide anion, we chose to monitor the level of H_2O_2 produced as a by-product of superoxide anion dismutation by SOD mimetics, in order to provide us with a reliable and reproducible assay format (see Equation 1). The long-lived stability of H_2O_2 ($t_{1/2} \geq 8$ h), was a crucial factor that allowed for the development of such an assay system.

This simple, relatively inexpensive, and reproducible assay was modeled after the development of SOD-immobilized biosensors created for electrochemical methods of detecting superoxide anion concentration by measuring H_2O_2 content.^[35] Our protocol was initially based on a procedure described by Pastor et al.,^[36] who measured SOD activity from native SOD enzyme embedded within collagen gels. In their system, superoxide anions were generated externally to the hydrogels using xanthine/xanthine oxidase and were catalytically degraded by the native SOD enzyme physically entrapped within the hydrogels to produce H_2O_2 . The level of H_2O_2 generated in this manner was then quantified by the standard Amplex Red detection methods.^[37] Unfortunately, we were unable to reproduce the results described by these investigators due to high levels of interference between the xanthine oxidase and Amplex Red reagents. We therefore modified and improved the basic system described by these investigators, creating a new, simple and robust assay format with the versatility to assess the activity of immobilized native SOD enzyme as well as immobilized SOD mimetics.

In the newly developed assay system, the NADH/PMS system was utilized for in situ superoxide anion generation.^[38–40] Diffusional limitations to the assay were minimized by polymerizing hydrogels as thin disks to maximize gel aspect ratios (diameter/height = 15:1), as well as by providing convectional forces to improve the transport of superoxide

anions into the hydrogels to come in contact with the polymerized MnTPPyP-Acryl. In addition, incubation of the hydrogels with NADH/PMS separately from Amplex Red and HRP provided for the maximum amount of H₂O₂ formed by superoxide anion dismutation while minimizing the exposure of NADH to HRP, which can result in the generation of excess H₂O₂ and skew results.^[41]

Results from this new solid phase assay to probe for SODm activity polymerized within hydrogels are shown in Figure 4. The SOD activity of hydrogels polymerized with varying mol% of MnTPPyP-Acryl were compared to control hydrogels polymerized with TPPyP-Acryl, which lacked the Mn metal ion coordinated in the porphyrin ring and should therefore be inactive. Fluorescence measurements from hydrogels containing only PEGDA were subtracted from measurements with polymerized porphyrins in order to remove interference from NADH and HRP interactions with the measurements; these measurements were then converted to H₂O₂ content by comparison to a calibration curve for H₂O₂ concentration. These results showed a dose-dependent increase in SOD activity with increasing quantities of MnTPPyP-Acryl polymerized within the hydrogels. Maximal activity was attained with hydrogels containing 0.1 and 0.25 mol% MnTPPyP-Acryl, whose values were statistically indifferent (*p*-value > 0.25). In contrast, only minimal levels of SOD activity were observed with control hydrogels containing any level of TPPyP-Acryl, indicating that the H₂O₂ formed by the hydrogels tested was indeed provided only by the active form of the SOD mimetic, and not solely due to the incorporation of any porphyrin molecules into the hydrogels. The decrease in SOD activity at 0.5 mol% MnTPPyP-Acryl may possibly be attributed to the slight catalase activity that Mn tetrapyrrolyl porphyrins exhibit,^[42] which would lead to decreasing H₂O₂ concentrations when high enough levels of SODm were incorporated into the hydrogels.

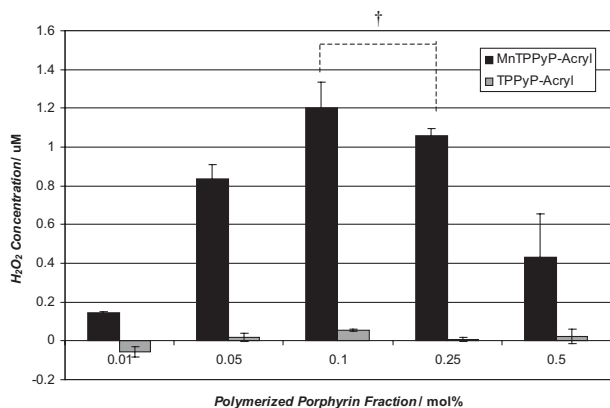


Figure 4. Solid-phase activity assay for PEGDA hydrogels containing polymerized MnTPPyP-Acryl utilizing Amplex Red detection of H₂O₂ formed from superoxide anion decomposition. PEGDA hydrogels were polymerized with from 0.01 to 0.25 mol% MnTPPyP-Acryl or TPPyP-Acryl. All sample conditions were tested with *n* = 3 replicates. † Denoted *p* > 0.05, indicating no statistical difference between results.

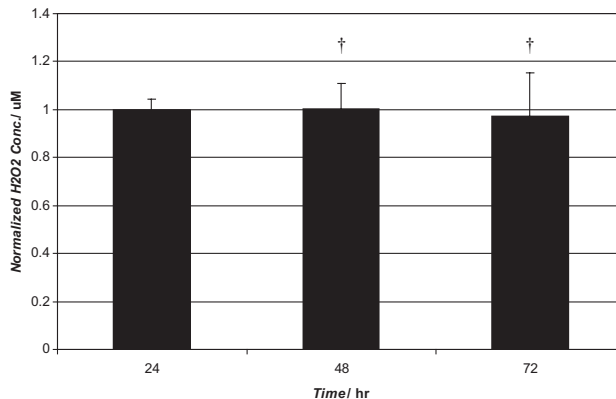


Figure 5. High levels of SOD activity maintained in PEGDA gels containing MnTPPyP-Acryl after repeated use in solid phase activity assays for up to 72 h post-polymerization. PEGDA hydrogels were prepared with 0.25 mol% MnTPPyP-Acryl, with *n* = 4 replicates. † Denoted *p* > 0.05, indicating no statistical difference between the results.

2.6. Repeated Use of PEGDA/SODm Hydrogels: Stability of the Functional Assay

The ability of PEGDA hydrogels containing MnTPPyP-Acryl to provide high levels of SOD activity over repeated use was tested during a 72 h period. PEGDA hydrogels containing 0.25 mol% MnTPPyP-Acryl were prepared, and the SOD activity of these hydrogels was tested daily during this time period. The results shown in Figure 5 indicate that essentially 100% of the original SOD activity 24 h post-polymerization was retained within these hydrogels after both 48 and 72 h. These data indicate that hydrogels prepared with SOD mimetics can provide consistent and multi-day activity with a single device, with the potential for longer-term activity. This prolonged activity illustrates both the durability of such a device as well as potential advantages over other systemic or controlled release delivery systems for SOD enzymes and mimetics, which will eventually result in depletion of the SOD therapeutic and necessitate repeated administration for those systems.

3. Conclusions

A polymerizable SODm, MnTPPyP-Acryl, was synthesized for incorporation into passive biomaterial scaffolds to provide active protection and mitigate damage from extracellularly secreted ROS to transplanted tissue, such as encapsulated pancreatic islets used for the treatment of T1DM. MnTPPyP-Acryl was shown to maintain an equivalent level of SOD enzymatic activity and comparable catalytic rate constant for the dismutation of superoxide anions when compared to MnTMPyP, a commercially available SODm. Photopolymerization of MnTPPyP-Acryl into PEGDA hydrogel constructs showed minimal interference/perturbation of the hydrogel structure when incorporated at low quantities, as evidenced by the similar crosslinking densities and crossover points between MnTPPyP-Acryl containing gels and blank PEGDA gels.

A new, simple and inexpensive solid-phase assay system was developed to test the activity of MnTPPyP-Acryl immobilized within PEGDA hydrogels. Traditional assays systems used to indirectly assay for superoxide anion concentration were incapable of assessing the activity of MnTPPyP-Acryl polymerized within the hydrogels, so an alternative assay method was developed, focusing on the detection and quantitation of H₂O₂ produced upon degradation of superoxide anions by the immobilized MnTPPyP-Acryl. Using this new assay system, we were able to demonstrate not only the ability of polymerized MnTPPyP-Acryl to dismutate superoxide anions but also the reusability of these hydrogel devices. The utility of creating polymerizable SOD mimetics lies in the versatility and general applicability that this class of therapeutic molecules may have to minimize inflammatory damage associated with general transplantation, and has the potential to be incorporated in any polymerizable medical device coatings to reduce inflammatory damage associated with biomaterial implantation.

4. Experimental

Materials: TPpP was purchased from Frontier Scientific (Logan, UT). 3-Iodopropanol was purchased from Trans World Chemicals, Inc. (Rockville, MD). Phenazine methosulfate was acquired from MP Biomedical (Solon, OH). Amplex Red and phosphate-buffered saline (PBS) were obtained from Invitrogen (Carlsbad, CA). Ammonium hexafluorophosphate (NH₄PF₆), tetrabutylammonium chloride (TBAC), triethylamine (TEA), manganese chloride tetrahydrate (MnCl₂·4H₂O), SOD enzyme, xanthine, xanthine oxidase, cytochrome *c*, β-nicotinamide adenine dinucleotide reduced disodium salt (NADH), and horseradish peroxidase (HRP) were purchased from Sigma-Aldrich (St. Louis, MO). The photoinitiator used in experiments, 1-[4-(2-hydroxyethoxy)-phenyl]-2-hydroxy-2-methyl-1-propane-1-one (I2959) was from Ciba Geigy (Newport, DE). All organic solvents were of ACS grade or better and were purchased from Sigma-Aldrich. PEGDA (MW = 10 000 g mol⁻¹) was synthesized as described previously [43].

Quarternization of TpyP: The pyridyl groups in TPpP (500 mg, 808 μmol) were quarternized with 3-iodopropanol (6.3 mL, 80 × eq.) in DMF for 24 h at 110 °C to synthesize meso-Tetra[1-(3-hydroxypropyl)-4-pyridyl] porphine (TPPyP-OH). Purification of TPPyP-OH followed standard procedures as described in the literature [44]. Briefly, the reaction mixture was added to chloroform (200 mL) and the quarternized porphyrin product was extracted into the water phase (3 × 200 mL). NH₄PF₆ (5 g) was added to precipitate the porphyrin from the water phase. The porphyrin precipitate was collected by centrifugation at 3000 × g and washed with 1:1 isopropanol/diethyl ether (3 × 100 mL). The solid precipitate was then desiccated to dryness. ¹H NMR (500 MHz, D₂O, 25 °C): δ = 9.4 (d, 8H, m-H), 9.0 (d, 16H, o-H, β-pyrrole), 5.1 (t, 8H, N⁺CH₂), 4.0 (m, 8H, N⁺CH₂CH₂), 2.6 (t, 8H, CH₂OH). Anal. calcd for TPPyP-OH(PF₆)₄ × 4H₂O (C₅₂H₆₂F₂₄N₈O₈P₄): C 41.44, H 4.15, N 7.44; found: C 41.14, H 3.93, N 7.11.

Acrylation of TPPyP-OH: The TPPyP-OH (PF₆⁻) salt (100 mg) was dissolved in acetone dried under molecular sieves and the hydroxyl moieties were acrylated by drop-wise addition with acryloyl chloride (0.045 mL, 8 × eq.) to the reaction mixture in the presence of TEA (0.078 mL, 8 × eq.) under argon in an ice-water bath to synthesize TPPyP-Acryl. Following acryloyl chloride addition, the reaction was allowed to warm to 20 °C and continued for an additional 24 h. The TPPyP-Acryl product was then precipitated from acetone by adding TBAC (5 g), and collected by centrifugation at 3000 × g. The product was washed with acetone (3 × 100 mL), the desiccated to

dryness. ¹H NMR (500 MHz, D₂O, 25 °C) δ = 9.5 (d, 8H, m-H), 9.1–9.2 (d, 16H, o-H, β-pyrrole), 6.5 (d, 1H, CH₂=CH), 6.0 (d, 1H, CH₂=CH), 6.3 (dd, 1H, CH₂=CH), 5.2 (t, 8H, N⁺CH₂), 4.6 (m, 8H, N⁺CH₂CH₂), 2.8 (t, 8H, CH₂OH). Anal. calcd for TPPyP-Acryl(PF₆)(Cl)₃ × 8H₂O (C₆₁H₇₆Cl₃F₆N₈O₁₅P): C 51.86, H 5.42, N 7.93; found: C 51.93, H 5.94, N 7.74.

Metallation of TPPyP-Acryl: Metallation of TPPyP-Acryl proceeded following standard procedures [45]. Briefly, TPPyP-Acryl (50 mg) and MnCl₂·4H₂O (200 mg, ~20 × eq.) were dissolved in dH₂O (10 mL) with 1 M NaOH (100 μL) and mixed at 20 °C to form MnTPPyP-Acryl. The degree of metallation was assessed by monitoring the Soret band shift from 424 to 463 nm, with complete metallation observed after approx. 24 h. The MnTPPyP-Acryl was then purified as described previously, with the addition of NH₄PF₆ to precipitate the metalloporphyrin, followed by 1:1 isopropanol/diethyl ether washes. Counterion exchange to Cl⁻ was then achieved by dissolving the product in acetone and metalloporphyrin precipitation upon the addition of TBAC. The final Cl⁻ form of MnTPPyP-Acryl was then desiccated to dryness overnight. Anal. calcd for Mn(III)TPPyP-Acryl(Cl)₅ × 8H₂O (C₆₁H₇₄Cl₅MnN₈O₁₅): C 52.65, H 5.36, N 8.05; found: C 53.16, H 5.66, N 7.98. UV/Vis (dH₂O) λ_{max} (ε) = 463 nm (145 000 M⁻¹ cm⁻¹).

Solution-Based Activity Assay: The solution-based ability of MnTPPyP-Acryl to degrade superoxide anions was monitored using a modified xanthine/xanthine oxidase assay initially described by McCord and Fridovich [30]. Native SOD enzyme (MW = 32.5 kDa), MnTMPyP or MnTPPyP-Acryl were incubated with xanthine (50 μM), xanthine oxidase (5 nM), and cytochrome *c* (10 μM) in sodium phosphate buffer (50 mM, pH 7.8) + 0.1 mM EDTA. Absorbance measurements at 550 nm were recorded for 2 min to measure the reduction of cytochrome *c* by chemically generated superoxide anions using a Lambda 40 UV/Vis Spectrometer (Perkin Elmer, Waltham, MA). These reagent concentrations used were chosen to provide a rate of increase in the A₅₅₀ of 0.025 AU min⁻¹ in the absence of SOD enzyme or SODm. One unit of SOD activity was therefore defined as the concentration of SOD or SOD mimetic required to inhibit the rate of cytochrome *c* reduction at 550 nm by 50% [30]. All conditions were tested in triplicate.

Polymerization of MnTPPyP-Acryl into PEGDA Hydrogel: 10 wt% (i.e., 10 mM) hydrogels containing PEGDA (MW = 10 000 g mol⁻¹) and MnTPPyP-Acryl (0–2 mol%) were dissolved in PBS and photopolymerized with I2959 (0.05 wt%) in custom cylindrical Teflon molds (6.35 mm diameter, 3.2 mm thick) for up to 20 min at 365 nm and ~10 mW cm⁻². Following polymerization, the hydrogels were soaked in PBS (0.5 mL) for a minimum of 1 h to remove any unreacted monomers from the gels.

Rheology Measurements for PEGDA/SODm Hydrogels: The shear modulus (*G*) and the crossover point for gelation, where the storage modulus (*G'*) and the viscous modulus (*G''*) intersect, were measured for thin (50 μm) PEGDA hydrogels containing MnTPPyP-Acryl (0–5 mol%) using a modified ARES rotational rheometer (TA Instruments, New Castle, DE), which allowed for real-time measurements during the photopolymerization process. Hydrogels were photopolymerized between 20 mm flat quartz plates using a Ultracure mercury arc lamp (100 W) with a liquid-filled light guide (EFOS, Inc., Ontario, Canada) and 365 nm bandpass filter to achieve a light intensity of ~10 mW cm⁻², until a stable *G'* value was obtained and where *G* ≈ *G'* when *G'* ≫ *G''*. The crosslinking density of the hydrogels, ρ_x, was calculated from *G'* measurements using Equation (3)

$$\rho_x = G' / (RTQ^{-1/3}) \quad (3)$$

where *R* is the gas constant, *T* the temperature, and *Q* the equilibrium volume swelling ratio with a theoretical value of 10.63 for 10 wt% PEG hydrogels [46].

Solid-Phase Activity Assay: A new solid-phase assay system was developed to detect the SOD activity level of MnTPPyP-Acryl

macromers polymerized into PEGDA hydrogel networks. Hydrogels (10 wt %) were prepared by photopolymerizing PEGDA solutions (20 μ L) containing MnTPPyP-Acryl or TPPyP-Acryl (0–0.5 mol%) with I2959 (0.05 wt%) in between glass slides using Teflon spacers (0.5 mm) for 10 min at 365 nm and ~ 10 mW cm⁻². The hydrogels were then placed in 48-well non-tissue culture treated polystyrene plates and allowed to swell in Tris–HCl buffer (50 mM, pH 8.0) for 30 min to allow for the removal of non-polymerized monomers. A solution (200 μ L) containing NADH (50 μ M) and PMS (0.25 μ M) was then added to the hydrogels, and the hydrogels were placed on an orbital shaker for 30 min to allow for H₂O₂ formation. A fraction of the NADH/PMS solutions (100 μ L) were then transferred to 96-well black plates and a solution (100 μ L) of Amplex Red (50 μ M) and HRP (0.2 U mL⁻¹) were added to the wells. The fluorescence generated from Amplex Red cleavage to resorufin due to the H₂O₂ generated in the presence of HRP was monitored using a Wallac Victor 2 1420 Multilabel Counter with 550 and 570 nm excitation and emission bandpass filters, respectively (Perkin-Elmer, Waltham, MA). All conditions were tested in triplicate.

Recurrent Use of PEGDA/MnTPPyP-Acryl Hydrogels: The ability of MnTPPyP-Acryl-containing hydrogels to provide adequate SOD activity over multiple discrete uses was assessed. Control and sample hydrogels containing PEGDA only or PEGDA polymerized with MnTPPyP-Acryl (0.25 mol%) were prepared as described above, respectively. The hydrogels were then soaked in Tris–HCl buffer (1 mL; 50 mM, pH 8.0) for 24 h at 4 °C with multiple buffer changes prior to assaying for SOD activity. The SOD activity of these hydrogels was assessed using the solid-phase assay system developed and described above. After each round of assays, the gels were soaked in Tris–HCl buffer solution to leach out any remaining NADH/PMS from within the gels during the interim 24 h period between assays at 4 °C. The buffer solutions were then removed and the same gels were once again ready for assaying for the next time point. Solid-phase assays on the gels proceeded at 24, 48, and 72 h post-polymerization, using $n = 4$ replicates. Fluorescence measurements were normalized to measurements obtained during the initial 24 h time point.

Received: April 25, 2008

Published online: October 6, 2008

- [1] E. J. Weringer, A. A. Like, *Am. J. Pathol.* **1986**, *125*, 107.
- [2] J. W. Yoon, H. S. Jun, P. Santamaria, *Autoimmunity* **1998**, *27*, 109.
- [3] E. Ho, T. M. Bray, *Proc. Soc. Exp. Biol. Med.* **1999**, *222*, 205.
- [4] D. Salvemini, D. P. Riley, S. Cuzzocrea, *Nat. Rev. Drug Discov.* **2002**, *1*, 367.
- [5] C. Muscoli, S. Cuzzocrea, D. P. Riley, J. L. Zweier, C. Thiemermann, Z. Q. Wang, D. Salvemini, *Br. J. Pharmacol.* **2003**, *140*, 445.
- [6] J. D. Piganelli, S. C. Flores, C. Cruz, J. Koepp, I. Batinic-Haberle, J. Crapo, B. Day, R. Kachadourian, R. Young, B. Bradley, K. Haskins, *Diabetes* **2002**, *51*, 347.
- [7] K. M. Faulkner, S. I. Liochev, I. Fridovich, *J. Biol. Chem.* **1994**, *269*, 23471.
- [8] R. F. Pasternack, A. Banth, J. M. Pasternack, C. S. Johnson, *J. Inorg. Biochem.* **1981**, *15*, 261.
- [9] L. Benov, I. Batinic-Haberle, *Free Radic. Res.* **2005**, *39*, 81.
- [10] K. Asayama, N. W. Kooy, I. M. Burr, *J. Lab. Clin. Med.* **1986**, *107*, 459.
- [11] B. Tyrberg, D. L. Eizirik, S. L. Marklund, B. Olejnicka, O. D. Madsen, A. Andersson, *Pharmacol. Toxicol.* **1999**, *85*, 269.
- [12] G. Papaccio, *Histol. Histopathol.* **1993**, *8*, 751.
- [13] A. Rabinovitch, W. L. Suarez-Pinzon, *Biochem. Pharmacol.* **1998**, *55*, 1139.
- [14] K. Grankvist, S. Marklund, I. B. Taljedal, *Nature* **1981**, *294*, 158.
- [15] F. Horio, M. Fukuda, H. Katoh, M. Petruzzelli, N. Yano, C. Rittershaus, S. Bonner-Weir, M. Hattori, *Diabetologia* **1994**, *37*, 22.
- [16] I. N. Nomikos, Y. Wang, K. J. Lafferty, *Immunol. Cell Biol.* **1989**, *67*, 85.
- [17] K. Grankvist, S. L. Marklund, *Int. J. Biochem.* **1986**, *18*, 109.
- [18] C. Y. Cheung, K. S. Anseth, *Bioconjug. Chem.* **2006**, *17*, 1036.
- [19] L. M. Weber, C. Y. Cheung, K. S. Anseth, *Cell Transplant.* **2008**, *16*, 1049.
- [20] M. Benaglia, T. Danelli, F. Fabris, D. Sperandio, G. Pozzi, *Org. Lett.* **2002**, *4*, 4229.
- [21] C. J. Rogers, T. J. Dickerson, P. Wentworth, K. D. Janda, *Tetrahedron* **2005**, *61*, 12140.
- [22] T. Tay, H. Turk, R. Say, *React. Funct. Polym.* **2007**, *67*, 999.
- [23] E. Hasegawa, J. I. Nemoto, T. Kanayama, E. Tsuchida, *Eur. Polym. J.* **1978**, *14*, 123.
- [24] A. Kajiwara, K. Aramata, M. Kamachi, K. Sumi, *Polym. J.* **1994**, *26*, 215.
- [25] M. Kamachi, X. S. Cheng, T. Kida, A. Kajiwara, M. Shibasaka, S. Nagata, *Macromolecules* **1987**, *20*, 2665.
- [26] E. Tsuchida, E. Hasegawa, T. Kanayama, *Macromolecules* **1978**, *11*, 947.
- [27] H. Kawakami, T. Ohse, M. Kawano, S. Nagaoka, *Polym. Adv. Technol.* **1999**, *10*, 270.
- [28] T. Ohse, H. Kawakami, A. Morita, S. Nagaoka, *J. Biomater. Sci. Polym. Ed.* **1999**, *10*, 917.
- [29] S. Asayama, K. Mizushima, S. Nagaoka, H. Kawakami, *Bioconjug. Chem.* **2004**, *15*, 1360.
- [30] J. M. McCord, I. Fridovich, *J. Biol. Chem.* **1969**, *244*, 6049.
- [31] S. S. Ali, J. I. Hardt, K. L. Quick, J. S. Kim-Han, B. F. Erlanger, T. T. Huang, C. J. Epstein, L. L. Dugan, *Free Radic. Biol. Med.* **2004**, *37*, 1191.
- [32] J. Butler, G. G. Jayson, A. J. Swallow, *Biochim. Biophys. Acta* **1975**, *408*, 215.
- [33] L. Packer, E. Cadenas, *Handbook of Synthetic Antioxidants*, M. Dekker, New York **1997**.
- [34] M. M. Tarpey, I. Fridovich, *Circ. Res.* **2001**, *89*, 224.
- [35] E. Emregul, *Anal. Bioanal. Chem.* **2005**, *383*, 947.
- [36] I. Pastor, R. Esquembre, V. Micol, R. Mallavia, C. R. Mateo, *Anal. Biochem.* **2004**, *334*, 335.
- [37] M. Zhou, Z. Diwu, N. Panchuk-Voloshina, R. P. Haugland, *Anal. Biochem.* **1997**, *253*, 162.
- [38] J. F. Ewing, D. R. Janero, *Anal. Biochem.* **1995**, *232*, 243.
- [39] M. Nishikimi, N. Appaji, K. Yagi, *Biochem. Biophys. Res. Commun.* **1972**, *46*, 849.
- [40] U. M. Rao, *Free Radic. Biol. Med.* **1989**, *7*, 513.
- [41] T. V. Votyakova, I. J. Reynolds, *Arch. Biochem. Biophys.* **2004**, *431*, 138.
- [42] B. J. Day, I. Fridovich, J. D. Crapo, *Arch. Biochem. Biophys.* **1997**, *347*, 256.
- [43] C. R. Nuttallman, M. C. Tripodi, K. S. Anseth, *J. Biomed. Mater. Res. A* **2004**, *68*, 773.
- [44] I. Batinic-Haberle, I. Spasojevic, P. Hambright, L. Benov, A. L. Crumbliss, I. Fridovich, *Inorg. Chem.* **1999**, *38*, 4011.
- [45] I. Batinic-Haberle, L. Benov, I. Spasojevic, I. Fridovich, *J. Biol. Chem.* **1998**, *273*, 24521.
- [46] C. N. Salinas, K. S. Anseth, **2008**, unpublished.